Clin. Lab. 2024;70:XXX-XXX

ORIGINAL ARTICLE

3D Culture System for Human Adrenal Glands That Uses a Sequential Processing Medium to Facilitate Cortical-Medullary Cell Development

Yajie Guo [1, *], Bingqian Guo [1, *], Yan Huang [2, *], Yu Ye [3, 4], Hongfei Chen [2], Liying Zhang [5], Minxi Li [5], Yifu Wang [1], Yufang Lv [1], Jinling Liao [1], Yang Chen [4], Yu Long [6], Jinghang Jiang [1], Zhongyuan Chen [1], Yi Guo [1], Zengnan Mo [1, 4], Yonghua Jiang [1, 5, 7]

[*] *These authors contributed equally to this work: Yajie Guo, Bingqian Guo, and Yan Huang*
[1] *Center for Genomic and Personalized Medicine, Guangxi Key Laboratory for Genomic and Personalized Medicine, Guangxi Collaborative Innovation Center for Genomic and Personalized Medicine, Guangxi Medical University, Nanning, China*
[2] *Department of Obstetrics, The Second Affiliated Hospital of Guangxi Medical University, Guangxi Medical University, Nanning, Guangxi, China*
[3] *Department of Urology, The Second Affiliated Hospital of Guangxi Medical University, Guangxi Medical University, Nanning, Guangxi, China*
[4] *Department of Urology, The First Affiliated Hospital of Guangxi Medical University, Nanning, Guangxi, China*
[5] *Department of Gynecology, The Second Affiliated Hospital of Guangxi Medical University, Guangxi Medical University, Nanning, Guangxi, China*
[6] *Department of Obstetrics, The First Affiliated Hospital of Guangxi Medical University, Nanning, Guangxi, China*
[7] *Life Sciences Institute, Guangxi Medical University, Nanning, Guangxi, China*

SUMMARY

Background: **The human adrenal gland is composed of the cortex and the medulla, which contain different function cells. The aim of this study was to build a 3D culture system for human adrenal glands.**
Methods: **Human fetal adrenal tissues were digested into a cell suspension culture and processed in three-phase 3D cultures.**
Results: **Apparent spheroids could be seen from the 4th day on. After 21 days of 3D culture, steroid synthesis cells were evident via CYP17A1+ immunohistochemical staining and flow cytometry analysis. Electron microscopy analysis showed that these cells were present in lipid droplets in the cytoplasm. Meanwhile, TH+ cells represented catecholamine-producing cells, and these cells exhibited electron density particle gathering in the cytoplasm. Dehydroepiandrosterone and epinephrine syntheses were further confirmed via enzyme-linked immunosorbent assay.**
Conclusions: **We established a 3D culture system for human adrenal glands by using a sequential processing medium to facilitate cortical–medullary cell development.**
(Clin. Lab. 2024;70:xx-xx. DOI: 10.7754/Clin.Lab.2024.240719)

Correspondence:
Zengnan Mo
Center for Genomic and Personalized Medicine
Guangxi Key Laboratory for Genomic and Personalized Medicine
Guangxi Collaborative Innovation Center for Genomic and Personalized Medicine
Guangxi Medical University
Nanning, 543002
China
Phone/Fax: + 86 07715641040
Email: mozengnan@gxmu.edu.cn
Yonghua Jiang
Center for Genomic and Personalized Medicine
Guangxi Key Laboratory for Genomic and Personalized Medicine
Guangxi Collaborative Innovation Center for Genomic and Personalized Medicine
Guangxi Medical University
Nanning, 543002
China
Phone/Fax: + 86 07715641040
Email: jiangyonghua@stu.gxmu.edu.cn

Manuscript accepted July 31, 2024

KEYWORDS

3D culture system, adrenal organoid, steroid hormone, catecholamine

INTRODUCTION

Human adrenal glands are essential parenchymal endocrine organs that consist of the cortex and the medulla, which develop from the mesoderm and the ectoderm. In adults, the adrenal gland cortex is subdivided into three distinct zones that secrete different steroid hormone, namely, mineralocorticoids for the *zona glomerulosa* (ZG), glucocorticoids for the *zona fasciculata* (ZF), and androgen precursors for the *zona reticularis* (ZR). The inner medulla chromaffin cells secrete catecholamine. The adult adrenal cortex undergoes rapid tissue renewal, accompanied by adrenal hormone day - night rhythms and short-term and long-term fluctuations throughout life [1,2]. Gene mutation or adrenal cortex dysfunction results in congenital adrenal hyperplasia, primary adrenal insufficiency, or adrenocortical hyperfunction (Cushing's syndrome) [3]. Furthermore, stem and progenitor cells under the cyst potential contribute to adrenocortical carcinomas [4,5]. Understanding how such disorders arise and how they can be treated requires suitable cell or animal models.

In recent years, the adrenal organoid was obtained from virus tissues and other species, including human, mouse, and bovine. This spheroid from human fetal adrenal glands retains cell viability and sustains high steroid-producing activity; it exhibits specific biological responses to adrenocorticotropic hormone (ACTH) stimulation [6,7]. Through stepwise culture, humans have induced pluripotent stem cells to differentiate into fetal-zone adrenal cortex-like cells, gaining steroid biosynthesis function [8]. Similarly, adrenal chromaffin-like cells diverge from human pluripotent stem cells [9] or H295R [10]. In addition, a more compressed organoid model of cortex–medulla interaction has been constructed from human benign adrenal tumors or bovine adrenal glands, which contain a variety of endocrine cells/tissues, including those of cortical and medullary origin [11]. Nevertheless, dehydroepiandrosterone (DHEA) production by ZR occurs only in humans and a few other primates, but not in mouse or bovine; hence, suitable cell and animal models of human adrenal disease are still lacking [12,13]. Therefore, focus on cultivating engineered organoids using advanced bioengineering tools for personalized tissue repair and biofunction reconstruction is required. The current study aimed to establish a 3D culture system for human fetal adrenal glands that exhibits steroid and catecholamine biosynthesis function.

MATERIALS AND METHODS

Human fetal samples

Human fetal adrenal tissues were collected from elective, non-medically motivated pregnancy terminations at different gestation weeks (GW) from June to December 2020, including three samples at 7 weeks, two samples at 8 weeks, and one sample each at 9, 12, and 13 weeks. The organs were too small; hence, primary cell populations were pooled together for further culture, and gender was not identified.

The study was approved by the Ethics Committee of the Second Affiliated Hospital of Guangxi Medical University (KY-0096) and is in compliance with the Declaration of Helsinki of the World Medical Association – ethical principles for medical research involving human subjects.

Isolation and expansion of fetal adrenal cells

Following fetal adrenal dissection and mesenchyme removal, the sample was digested with 0.1 mg/mL [10] TL (5401020001, Roche) and 1 mg/mL DNase I (10104159001, Roche) in RPMI 1640 (C11875500BT, Gibco) for 20 minutes at 37°C with gentle shaking throughout. The enzyme was inactivated by RPMI 1640 with 10% fetal bovine serum (FBS) (21700075, Gibco; 3007.03, HyClone). The suspension culture was then filtered through a 100 μm cell strainer (352360, Falcon), washed twice with Dulbecco's phosphate-buffered saline (D-PBS), and spun for 5 minutes at 300 g. Then, the cells were resuspended and counted.

To ensure that cells from all stages of embryonic development were included, the primary cell populations from the 7-, 8-, 12-, and 13-week fetal adrenal cells were mixed. Then, 1×10^5 cells were seeded into 35 mm dishes (430165, Corning) with Dulbecco's Modified Eagle's Medium (DMEM)/F12 (12634010, Life Technologies) that contained 10% FBS and 2 mM of L-glutamine (25030081, Gibco) and cultured at 37°C in a humidified 5% CO_2 atmosphere. Primary cells were cultured for 7 days, passaged with trypsin 1 or 2 times.

3D culture system

The expanded adherent cells were suspended as 1,000 cells/drops in a low attachment surface plate (3471, Corning) coated with growth factor reduced Matrigel (356231GFR-Matrigel, Corning), diluted 1/20 in DMEM/F12 (12634010, Life Technologies). The cells were cultured in 3D throughout all the phases of the protocols. Phase 1: DMEM/F12 medium supplemented with 1X N2 (17502048, Life Technologies), 1X B-27 supplement minus vitamin A (12587010, Life Technologies), 2 mM of L-glutamine, 100 ng/mL of FGF2 (100-18C, Peprotech), 100 μg/mL of primocin (ant-pm-1, Invivogen), 500 nM of ALK-4, -5, -7 inhibitor A83-01 (2939, Tocris), and 10 μM of ROCK inhibitor Y-27632 (688000, Millipore). Phase 2: Phase 1 medium added with 1.5 μM of CHIR99021, 5 ng/mL of recombinant human R-spondin1 (4645-RS, Bio R&DTechne),

and 200 nM of ACTH (12279-41-3, MedChemExpress). Phase 3: Phase 2 medium with 500 pg/mL of BMP4 (314-BP-010, R&D Systems).

Immunofluorescence staining

The organoids were fixed overnight in 4% paraformaldehyde, then paraffin-embedded. The organoids were cut in 4 μm formalin-fixed tissue sections. Primary antibodies: mouse anti-human CYP17A1 primary antibodies (1:100, sc-374244, Santa). Secondary antibodies: Alexa Fluor 594-conjugated donkey anti-mouse IgG (1:500, ab150112, Abcam). Fluorescence images were captured by using a laser scanning confocal microscope (TCS SP8, Laika Microscope System Shanghai Trading Co., Ltd.).

Flow cytometry analysis

The organoids were dissociated into single cells. Intracellular staining permeabilization wash buffer (10X, 421002, Biolegend) was used in accordance with the manufacturer's instructions. Briefly, the samples were incubated in Perm/Wash buffer with primary antibodies against SF-1 (1:50, sc-393592, Santa), CYP17A1 (1:50, sc-374244, Santa), and TH (1:50, sc-374047, Santa) for 20 minutes at room temperature. The samples were washed with Perm/Wash buffer, resuspended in PBS (with 1% BSA), and incubated with Alexa Fluor 488-conjugated goat anti-mouse IgG secondary antibodies (1:1,000, ab150117, Abcam) for 20 minutes at room temperature. FACS Diva software version 8.0.1 (BD Biosciences) was used with FACS C6 (BD Biosciences) for the cell sorting experiments. FlowJo software version 10 was used to analyze the data.

Electron microscopy

The samples were endorsed to Servicebio Co. A simplified overview was listed, tissue cell samples were sectioned by resin embedding, 60 - 80 nm ultra-thin sections stained with lead and uranium, and then magnification imaging by transmission electron microscope (HT7700, Hitachi).

RNA sequencing and analysis

All the samples (Phases 1, 2, and 3) were collected and lysed in TRIzol reagent and stored at -80°C until use. RNA sequencing was performed by the Novogene Co. The library preparations were sequenced on an Illumina NovaSeq platform, and 150 bp paired-end reads were generated. FeatureCounts.v1.5.0-p3 was used to count the read numbers mapped to each gene. Then, the fragments per kilobase of feature per million mapped reads (FPKM) value of each gene was calculated based on the length of the gene and read count mapped to the gene. Differential expression analysis was performed using the DESeq2 R package (1.16.1). The three groups of samples were compared for the differential expression analysis, and the first 50 genes with a high expression in each sample were used for gene heat mapping by R (version 3.0.3) ggplot2 package and the pheatmap package. Gene Ontology (GO) and Kyoto Encyclopedia of Genes and Genomes analyses were used to detect the differences in gene function expression among cell clusters. Terms with a p-value < 0.05 were considered significantly enriched.

Hormone quantification

Conditioned media were collected from the organoid cultures, centrifuged to remove debris, and stored at -80°C until use. Following the manufacturer's instructions, DHEA (KJ-0766), epinephrine (EPI, KJ-0751), noradrenaline (NA, KJ-0995), dopamine (DA, KJ-1008), and cortisol (KJ-0076) enzyme-linked immunosorbent assays (ELISAs) (Jiangsu Kejing Biological Technology) were performed. OD value (450 nm) was measured by using an EPOCH2 microplate reader (Gen-5TSCHS2.06 software). The concentration of hormones in the supernatants was calculated from the line formula of the standard plots in GraphPad Prism 8.0.1.

Quantitative reverse transcription-polymerase chain reaction (qRT-PCR)

Total RNA was isolated using the HiPure Universal RNA Kit (Magen) and reverse transcription was performed using the PrimeScript RT Master Mix (TAKARA). qRT-PCR was conducted using a Roche Light Cycler 96 and FastStart Essential DNA Green Master kit in accordance with the manufacturer's instructions for all the genes. The primers used are listed in Supplementary Table 1. The qRT-PCR analyses were performed in triplicate, and Ct values were normalized against the internal control gene GAPDH. Fold differences in expression levels were calculated in accordance with the comparative Ct method.

Statistical analysis

Statistical tests were performed using GraphPad Prism. All the experiments were performed in three biological replicates. The results were expressed as the mean ± SD. Differences were assessed via a two-way ANOVA or Student's two-tailed unpaired *t*-test. p-values less than 0.05 were considered significant. Significance was defined as $*p < 0.05$, $**p < 0.01$, and $***p < 0.001$.

RESULTS

3D culture system of dissociated cells from human fetal adrenal glands

First, primary cells were seeded on and cultured for 7 days. Then, these cells were digested and replated in Matrigel (counted as Day 0) for organotypic culture until Day 21. Phase 1 medium contained B27, N2, A83-01, and Y-27632 (Days 0 to 8). Phase 2 medium added FGF2, CHIR99021, R-spondin1, and ACTH (Days 9 to 12), with the active FGF, WNT, and PKA signaling pathways to generate steroidogenic cells. To further drive adrenomedullary maturation, we added BMP-4 in Phase 3, which promoted chromaffin cell maturation

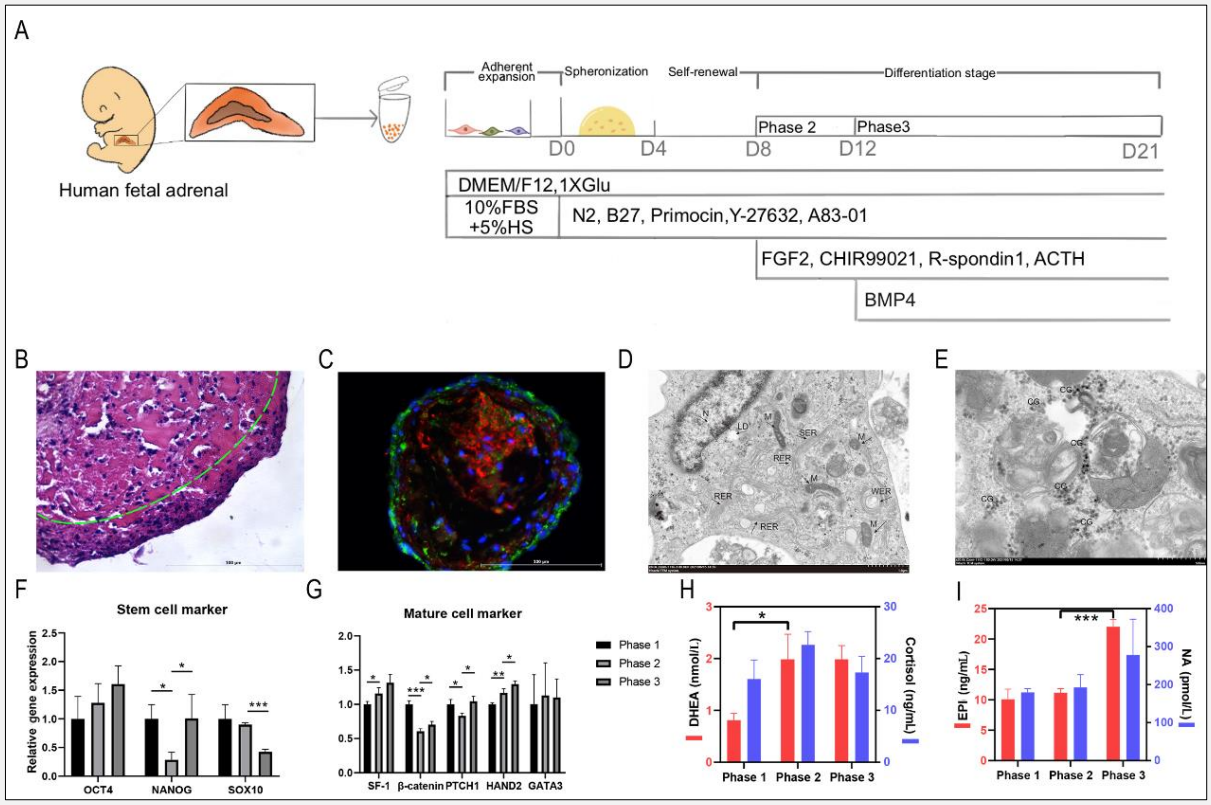

Figure 1. Characterization of adrenal gland organoids.

A) Outline of the culture protocol highlighting the order and timing of adrenal organoid development. B) HE staining of the adrenal spheroids (Phase 2); green line divides outer compact layer and inner loose layer. C) Immunofluorescence analysis of adrenal spheroids (Phase 2); NOV+ (green), CYP17A1+ (red), DAPI+ (blue). TEM images of D) steroidogenic cells (Phase 2), rough endosome reticulum (RER), smooth endoplasmic reticulum (SER), plentiful mitochondria (M), lipid droplets (LD), and E) chromaffin cells (Phase 3) chromaffin granules (GCs). qRT–PCR analysis F) stem cell markers and G) mature cell markers. ELISA analysis of hormone levels in cell culture medium H) cortisol and DHEA and I) EPI and NA. *p < 0.05; **p < 0.01; ***p < 0.0001.

(Days 13 to 21) (Figure 1A).

The number of spheroids increased sharply while forming the spheroids with 3 - 5 cell aggregates. Apparent spheroids could be seen from the 4th day on in 3D culture. The diameter of the spheroid continued to increase, reaching about 400 μm in the latter part of Phase 3 (Figure S1A, B).

Characterization of adrenal organoid development and differentiation

To identify the characteristics of different phase cells, histopathology, scanning electron microscopy, and flow cytometry analyses were performed. The spherical structure appeared in Phase 1, enlarged and remained during the entire culture progress. In Phase 3, the ribbon structure was visible via hematoxylin and eosin (HE) staining analysis (Figure 1B). With different medium ingredients for the three phases, the cell characteristics exhibited minimal distinction. The numbers of CD44+, CYP17A1+, S100B+, and TH+ cells were quantified via flow cytometry analysis, which showed that the CYP17A1+ percentages gradually increased from Phase 1. TH+ percentages were higher in Phase 3, relative to those in Phase 2 (Figure S1C).

After 21 days of 3D culture, the adrenal spheroids were harvested. NOV+ and CYP17A1+ cells were confirmed via immunofluorescence analysis (Figure 1C). Transmission electron microscopy (TEM) found smooth endoplasmic reticulum (SER), abundant mitochondria (M), and lipid droplets (LD) in the plasma, similar to mature steroidogenic cells (Figure 1D). Abundant electron density particles (chromaffin granules, CGs) were also found (Figure 1E). Some pluripotent, steroid function related genes were detected via qRT-PCR (Figure 1F, G). Compared with that in Phase 1, the gene expression of the stem cell-related gene NANOG was down-

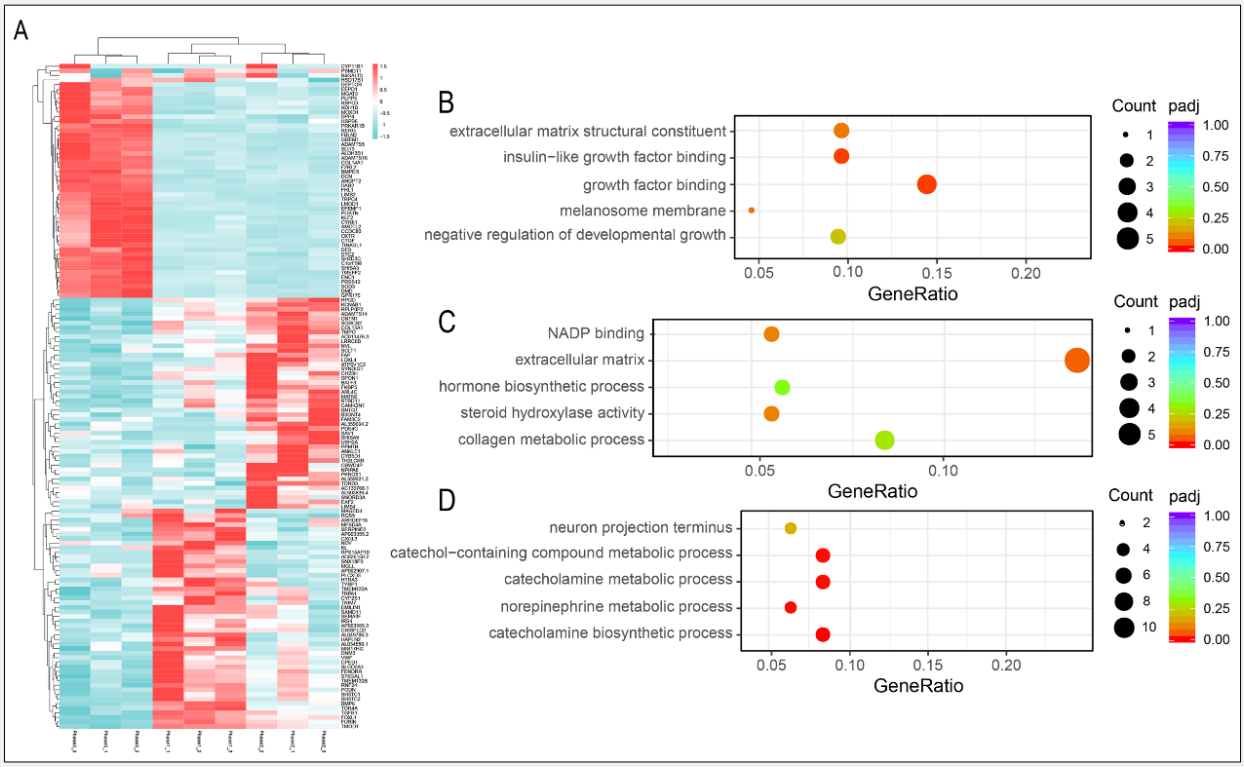

Figure 2. RNA-seq analysis of different stages of adrenal organoids. Top 145 highest genes of the 3 different phases. (A) Heat map analysis. GO enrichment analysis of (B) Phase 1, (C) Phase 2, and (D) Phase 3.

regulated in Phase 2, while the adrenal key functional gene SF1 was upregulated as steroid functional cells developed. Compared with that in Phase 2, the gene HAND2 (a marker of sympathoadrenal progenitors, SAPs) was upregulated in Phase 3, along with SOX10 (a marker of neural crest progenitor cells). Finally, ELISA analysis confirmed the steroid hormone DHEA and EPI in Phases 2 and 3 (Figure 1H, I).

Comparison of the differentiation stages via RNA-Seq for adrenal organoids

To further characterize the adrenal organoids, RNA-Seq was performed during the three phases. A total of 29,500 genes were detected and selected for subsequent analysis. Three groups from Phases 1, 2, and 3 were compared. The top 145 genes were taken to generate a gene heat map (Figure 2A). Gene heat map clustering showed that each phase clustered well among individuals, but Phases 1 and 2 exhibited better clustering than Phase 3. In accordance with organoid sphere formation and rapid cell proliferation and aggregation, MAGED4, SLCO3A1, and TBGB1 genes associated with active cell proliferation were highly expressed in Phase 1. Other genes associated with cell adhesion and the intercellular matrix, such as CNTN1, COL15A1, FAP, and SPON1, were also highly expressed in this phase. As more steroid synthesis cells matured in Phase 2, the ARL4C gene, which is involved in cholesterol and lipid metabolism, was highly expressed. Phase 3 is the last stage of 3D culture. In this stage, the cells become functional, with increased secretion and slower growth. The performances of RERG and DEPTOR, which inhibit cell proliferation and tumor formation negative regulation of protein kinase activity, and those of the neuroendocrine genes MOXD1 and TRPC4, were progressively upregulated.

Dot plots separately display the top 50 gene GO enrichment analyses. The Phase 1 pathway enriched in the extracellular matrix structural constituents suggests that this stage benefits the structure of the adrenal spheroids. In addition, melanosome aggregation and insulin-like growth factor positive regulation of development growth pathways occurred in Phase 1 (Figure 2B). Meanwhile, NADPH binding, steroid hydroxylase activity, and hormone biosynthetic process pathways were assembled in Stage 2, suggesting that the spheroids cells differentiated toward a steroidogenesis adrenal fate (Figure 2C). Sympathetic pathways were activated in

Phase 3 with the development of chromaffin cells and the synthesis of catecholamines (Figure 2D).

DISCUSSION

Based on their adjacent position, the adrenal cortex and medulla influence each other's function and structure through endocrine and paracrine effects. Our method takes advantage of the stepwise induced strategy. We activated the Wnt signaling pathway via CHIR99021 and R-spondin1 in Phase 1. Early adrenal development Wnt/β-catenin signaling plays an important role in the centripetal renewal of the cortex by inhibiting fascicular differentiation and promoting the undifferentiated state of progenitor cells [14], regulating morphogenesis by inducing the paracrine factors that directly affect cell migration, adhesion, and polarity [15]. As predicted, the spheroids grew quickly in size over time, as showed after 4 days in 3D culture. The transcript sequence GO analysis shows the extracellular matrix structural constituents in Phase 1. The extracellular matrices fibronectin and laminin are proven to help adrenocortical cells adhere and migrate [16]. Collagen IV is involved in the adrenal ACTH stimulation of DHEA and cortisol secretion [17].

Next, we appended FGF and ACTH in Phase 2, further promoting and maintaining cortical cell growth and proliferation. FGF2 is the most important subtype of the FGF family in adrenal glands. FGFR2 ligands were detected in human fetal or adult adrenal capsule and the cortex [18,19]. Mice with conditional deletion Fgfr2 exhibited severely hypoplastic adrenal glands around birth [20]. In addition, ACTH could accelerate ZG and ZF identity via the cAMP/PKA pathway, promoting glucocorticoid and androgen syntheses [17,21]. As indicated by the flow cytometry result, stem cell capsular (NOV+) cells decreased, while steroidogenic cells (CYP17A1+) increased. DHEA synthesis was further confirmed via ELISA. We believe that after the Phase 2 culture, functional steroid cells were successfully induced, and glucocorticoid microenvironment was created.

BMP4 was applied in Phase 3 to further drive adrenomedullary maturation. BMP4 not only induced sympathoadrenal (SA) cells at the dorsal aorta and within the adrenal gland, but also promoted chromaffin cell maturation [22,23]. Glucocorticoid and DHEA are regularly used as adrenal medullar culture media. Corticosteroid mimetic induced these cells to upregulate the chromaffin cell-specific marker for generating adrenal chromaffin-like cells from human pluripotent stem cells [22]. DHEA is helpful in bovine adrenal medulla spherical cultures [24]. In contrast with the previous cultivation methods, glucocorticoid and DHEA were self-synthesized instead of added.

However, this study has many limitations. Based on the limited fetal adrenal cell origin, we pooled adrenal glands for digested primer cells regardless of gender. The adrenal gland is a sexually dimorphic organ [3,25], and thus, this operation affects the accuracy of the sphere character analysis. Moreover, we did not sort stem cells or progenitor cells for culture. To provide a better induction culture scheme and a more proliferative spherical culture, separating pure stem cells, such as SF-1 + cells and SHH+ cells, may be necessary [26,27].

In conclusion, we established a 3D culture system for human adrenal glands that is a valuable preliminary model for investigating the development and homeostasis of the adrenal gland.

Source of Funds:

This work was supported by the Natural Science Foundation of China (82270806), Guangxi Key Research and Development Project (GuikeAB21196022, GuikeAA22412, and GuikeAA22398), Major Project of Guangxi Innovation Driven (AA18118016), the Natural Science Foundation of Guangxi Zhuang Autonomous Region (2021JJA140912 and 2020GXNSFDA297024), Major Project of Scientific Research and Technology Development Plan of Nanning (20221023), self-funded scientific research project of Guangxi Health Commission (Z-A20220479), and through the Medical Excellence Award funded by the Creative Research Development Grant from the First Affiliated Hospital of Guangxi Medical University (201903).

Ethical Approval:

This study was reviewed and approved by the regional Ethics Committee of the Second Affiliated Hospital of Guangxi Medical University (KY-0096).

Declaration of Interest:

The authors declare that they have no conflicts of interest.

References:

1. Ishimoto H, Jaffe RB. Development and function of the human fetal adrenal cortex: a key component in the feto-placental unit. Endocr Rev 2011;32(3):317-55. (PMID: 21051591)

2. Bechmann N, Berger I, Bornstein SR, Steenblock C. Adrenal medulla development and medullary-cortical interactions. Mol Cell Endocrinol 2021;528:111258. (PMID: 33798635)

3. Lyraki R, Schedl A. Adrenal cortex renewal in health and disease. Nat Rev Endocrinol 2021;17(7):421-34. (PMID: 34011989)

4. Kastriti ME, Kameneva P, Adameyko I. Stem cells, evolutionary aspects and pathology of the adrenal medulla: A new developmental paradigm. Mol Cell Endocrinol 2020;518:110998. (PMID: 32818585)

5. Scriba LD, Bornstein SR, Santambrogio A, et al. Cancer Stem Cells in Pheochromocytoma and Paraganglioma. Front Endocrinol (Lausanne) 2020;11:79. (PMID: 32158431)

6. Melau C, Nielsen JE, Perlman S, et al. Establishment of a Novel Human Fetal Adrenal Culture Model that Supports de Novo and Manipulated Steroidogenesis. J Clin Endocrinol Metab 2021; 106(3):843-57. (PMID: 33212489)

7. Poli G, Sarchielli E, Guasti D, et al. Human fetal adrenal cells retain age-related stem- and endocrine-differentiation potential in culture. FASEB J 2019;33(2):2263-77. (PMID: 30247985)

8. Sakata Y, Cheng K, Mayama M, et al. Reconstitution of human adrenocortical specification and steroidogenesis using induced pluripotent stem cells. Dev Cell 2022;57(22):2566-83.e8. (PMID: 36413950)

9. Ruiz-Babot G, Balyura M, Hadjidemetriou I, et al. Modeling Congenital Adrenal Hyperplasia and Testing Interventions for Adrenal Insufficiency Using Donor-Specific Reprogrammed Cells. Cell Rep 2018;22(5):1236-49. (PMID: 29386111)

10. Martinelli S, Cantini G, Propato AP, et al. The 3D in vitro Adrenoid cell model recapitulates the complexity of the adrenal gland. Sci Rep 2024;14(1):8044. (PMID: 38580769)

11. Bornstein S, Shapiro I, Malyukov M, et al. Innovative multidimensional models in a high-throughput-format for different cell types of endocrine origin. Cell Death Dis 2022;13(7):648. (PMID: 35879289)

12. Abbott DH, Bird IM. Nonhuman primates as models for human adrenal androgen production: function and dysfunction. Rev Endocr Metab Disord 2009;10(1):33-42. (PMID: 18683055)

13. Jin H, Xue Z, Liu J, Ma B, Yang J, Lei L. Advancing Organoid Engineering for Tissue Regeneration and Biofunctional Reconstruction. Biomater Res 2024;28:0016. (PMID: 38628309)

14. Walczak EM, Kuick R, Finco I, et al. Wnt signaling inhibits adrenal steroidogenesis by cell-autonomous and non-cell-autonomous mechanisms. Mol Endocrinol 2014;28(9):1471-86. (PMID: 25029241)

15. Mariani FV, Fernandez-Teran M, Ros MA. Ectoderm-mesoderm crosstalk in the embryonic limb: The role of fibroblast growth factor signaling. Dev Dyn 2017;246(4):208-16. (PMID: 28002626)

16. Feige JJ, Keramidas M, Chambaz EM. Hormonally regulated components of the adrenocortical cell environment and the control of adrenal cortex homeostasis. Horm Metab Res 1998;30(6-7):421-5. (PMID: 9694573)

17. Chamoux E, Bolduc L, Lehoux JG, Gallo-Payet N. Identification of extracellular matrix components and their integrin receptors in the human fetal adrenal gland. J Clin Endocrinol Metab 2001; 86(5):2090-8. (PMID: 11344212)

18. Guasti L, Candy Sze WC, McKay T, Grose R, King PJ. FGF signalling through Fgfr2 isoform IIIb regulates adrenal cortex development. Mol Cell Endocrinol 2013;371(1-2):182-8. (PMID: 23376610)

19. Leng S, Pignatti E, Khetani RS, et al. β-Catenin and FGFR2 regulate postnatal rosette-based adrenocortical morphogenesis. Nat Commun 2020;11(1):1680. (PMID: 32245949)

20. Häfner R, Bohnenpoll T, Rudat C, Schultheiss TM, Kispert A. Fgfr2 is required for the expansion of the early adrenocortical primordium. Mol Cell Endocrinol 2015;413:168-77. (PMID: 26141512)

21. Ruggiero C, Lalli E. Impact of ACTH Signaling on Transcriptional Regulation of Steroidogenic Genes. Front Endocrinol (Lausanne) 2016;7:24. (PMID: 27065945)

22. Abu-Bonsrah KD, Zhang D, Bjorksten AR, Dottori M, Newgreen DF. Generation of Adrenal Chromaffin-like Cells from Human Pluripotent Stem Cells. Stem Cell Reports 2018;10(1):134-50. (PMID: 29233551)

23. Unsicker K, Huber K, Schober A, Kalcheim C. Resolved and open issues in chromaffin cell development. Mech Dev 2013; 130(6-8):324-9. (PMID: 23220335)

24. Chung K-F, Qin N, Androutsellis-Theotokis A, Bornstein SR, Ehrhart-Bornstein M. Effects of dehydroepiandrosterone on proliferation and differentiation of chromaffin progenitor cells. Mol Cell Endocrinol 2011;336(1-2):141-8. (PMID: 21130143)

25. Dumontet T, Sahut-Barnola I, Septier A, et al. PKA signaling drives reticularis differentiation and sexually dimorphic adrenal cortex renewal. JCI Insight 2018;3:(2):e98394. (PMID: 29367455)

26. Grabek A, Dolfi B, Klein B, Jian-Motamedi F, Chaboissier M-C, Schedl A. The Adult Adrenal Cortex Undergoes Rapid Tissue Renewal in a Sex-Specific Manner. Cell Stem Cell 2019;25(2): 290-6.e2. (PMID: 31104943)

27. Kim AC, Barlaskar FM, Heaton JH, et al. In search of adrenocortical stem and progenitor cells. Endocr Rev 2009;30(3):241-63. (PMID: 19403887)

Additional material can be found online at:
http://supplementary.clin-lab-publications.com/240719/